

## Mice lacking the transcriptional corepressor TIF1 $\beta$ are defective in early postimplantation development

Florence Cammas, Manuel Mark, Pascal Dollé, Andrée Dierich, Pierre Chambon\* and Régine Losson

Institut de Génétique et de Biologie Moléculaire et Cellulaire, CNRS/INSERM/ULP/Collège de France, BP 163, 67404 Illkirch-Cedex, France

\*Author for correspondence (e-mail: chambon@igbmc.u-strasbg.fr)

Accepted 17 April; published on WWW 13 June 2000

### SUMMARY

**TIF1 $\beta$ , a member of the transcriptional intermediary factor 1 family, has been reported to function as a corepressor for the large class of KRAB domain-containing zinc finger proteins of the Krüppel type. To address the biological function of TIF1 $\beta$ , we have generated TIF1 $\beta$ -deficient mice by gene disruption. TIF1 $\beta$  protein was detected in wild-type but not TIF1 $\beta^{-/-}$  blastocysts. Homozygous mutant embryos, which developed normally until the blastocyst stage and underwent uterine**

**implantation, were arrested in their development at the early egg-cylinder stage at about embryonic day (E) 5.5 and were completely resorbed by E8.5. Taken together, these results provide genetic evidence that TIF1 $\beta$  is a developmental regulatory protein that exerts function(s) essential for early postimplantation development.**

Key words: TIF1 gene family, Heterochromatin-mediated silencing, KRAB domain, Gene disruption, Early lethality, Gastrulation, Mouse

### INTRODUCTION

Transcriptional repression plays a central role in a variety of developmental and differentiation processes from yeast to mammals (reviewed in Gray and Levine, 1996; Ip and Hemavathy, 1997; Ogbourne and Antalis, 1998). Accordingly, numerous important developmental regulatory genes have been identified that encode sequence-specific transcriptional repressors (Carroll, 1990; Schoenherr and Anderson, 1995; Gray and Levine, 1996; Zazopoulos et al., 1997; Fisher and Caudy, 1998 and refs therein). These regulatory proteins typically contain a DNA-binding domain (DBD) and one or more repression domains, which can exert their repressing effects through interactions with transcriptional intermediary factors (TIFs), whose ultimate function is to remodel chromatin structure (Kornberg and Lorch, 1999), to inhibit (pre)initiation complex formation (Orphanides et al., 1996), or to associate target genes with specialized nuclear compartments that confer transcriptional repression (Cockell and Gasser, 1999 and refs therein).

The KRAB (Krüppel-associated box) domain, which is present in about one third of the 300-700 human zinc-finger proteins (ZFPs) of the Krüppel type (Bellefroid et al., 1991), is one of the most widely distributed transcriptional repression domains yet identified in mammals (Margolin et al., 1994; Witzgall et al., 1994). When fused to a heterologous DBD, this regulatory domain of approx. 75 amino acids silences both basal and activated transcription in transfected cells, in a dose-dependent manner and over large distances (Pengue et al., 1994; Deuschle et al., 1995; Moosmann et al., 1997). Insight into the molecular mechanism(s) underlying this silencing

activity came from the recent identification of a nuclear protein, TIF1 $\beta$ , also named KAP-1 (Friedman et al., 1996) or KRIP-1 (Kim et al., 1996), which exhibits all the hallmarks of being a corepressor for the large family of KRAB-ZFPs; TIF1 $\beta$  was demonstrated to interact through a KRAB box (see Fig. 1B) with several different KRAB domains but not KRAB mutants deficient in repression, to enhance KRAB-mediated repression and to repress transcription when directly tethered to DNA (Friedman et al., 1996; Kim et al., 1996; Moosmann et al., 1996; Agata et al., 1999; Nielsen et al., 1999).

On the basis of sequence homologies, TIF1 $\beta$  was also identified as a member of the transcriptional intermediary factor 1 (TIF1) family (Le Douarin et al., 1996). In addition to TIF1 $\beta$ , the family includes TIF1 $\alpha$ , a putative nuclear receptor cofactor (Le Douarin et al., 1995, 1996; Zhong et al., 1999), and TIF1 $\gamma$ , whose function is unknown (Venturini et al., 1999). These three proteins are defined by the presence of two conserved amino acid regions: an N-terminal RBCC (RING finger, B boxes, coiled coil) motif, which may be involved in intermolecular interactions that influence the targeting to (and/or assembly of) subnuclear structures (Saurin et al., 1996; Boddy et al., 1997), and a C-terminal region containing a PHD finger and a bromodomain (see Fig. 1B). These latter two motifs are often associated and are present in a number of transcriptional cofactors acting at the chromatin level (Aasland et al., 1995; Jeanmougin et al., 1997 and refs therein). Interestingly, the bromodomain interacts with lysine-acetylated peptides derived from histones H3 and H4, suggesting a chromatin-targeting function for this highly conserved domain (Dhalluin et al., 1999; Winston and Allis, 1999).

Supporting the notion that TIF1 $\beta$  may exert its corepressor

function by a chromatin-mediated mechanism, TIF1 $\beta$  is known (1) to be associated with members of the heterochromatin protein 1 (HP1) family (Nielsen et al., 1999), a class of nonhistone proteins with a well-established function in heterochromatin-mediated silencing in *Drosophila* (Eissenberg et al., 1995; Elgin, 1996 and refs therein), (2) to phosphorylate HP1 proteins, to which it binds directly through a HP1 box (see Fig. 1B) (Le Douarin et al., 1996; Nielsen et al., 1999; Ryan et al., 1999) and (3) to possess an HP1-dependent and Trichostatin A (TSA; a specific inhibitor of histone deacetylase)-sensitive repression function (Nielsen et al., 1999). Thus, TIF1 $\beta$  may mediate the repression function of the KRAB domain by an epigenetic mechanism, which involves HP1 interaction and histone deacetylation, to induce formation of (and/or juxtaposition with) heterochromatin (Nielsen et al., 1999; Ryan et al., 1999).

To elucidate the physiological functions of TIF1 $\beta$ , we generated TIF1 $\beta$ -deficient mice. Null mutants develop normally to the blastocyst stage and implant, but fail to gastrulate, indicating that TIF1 $\beta$  is essential for early postimplantation mouse development.

## MATERIALS AND METHODS

### Construction of the targeting vector

To generate the TIF1 $\beta$  targeting vector, a 7-kb genomic fragment from the mouse TIF1 $\beta$  locus (F. Cammas, J.-M. Garnier, P. Chambon and R. Losson, unpublished) was used (see Fig. 1A). A 395-bp EcoRI-XhoI TIF1 $\beta$  fragment containing the 3' 377 bp of intron 3 and the 5' 18 bp of exon 4 was inserted between EcoRI and XhoI sites in pKSM3 (modified from pBluescript SK<sup>+</sup>, and containing a ClaI-AatII-XhoI-EcoRI-NotI-ClaI polylinker) to generate pTIF1B3. pTIF1B3 was digested with HindIII removing 43 bp in intron 3, which were replaced with a floxed PGK-Neo cassette (PGK-NeoLS5), to generate pTIF1B8. To create the 5' homologous arm, a 3-kb EcoRI TIF1 $\beta$  genomic fragment containing exons 1 to 3 and the 5' sequences of intron 3 (see Fig. 1A), was subcloned into the EcoRI site of pTIF1B8, yielding pTIF1B11. A 4.5-kb XhoI fragment 3' downstream to position 18 of exon 4 (see Fig. 1A), was inserted into the XhoI site of pKSM3, to generate pTIF1B4. A double-stranded oligonucleotide containing a loxP site (underlined), a BamHI site immediately downstream of the loxP site, and HindIII overhangs was produced by annealing two synthetic oligonucleotides WV144 (5'-AGCTA-TCATAACTTCGTATAATGTATGCTATACGAAGTTATGGATCCG-3') and WV255 (5'-AGCTCGGATCCATAACTTCGTATAGCAT-ACATTATACGAAGTTATGAT-3'), and was cloned into intron 14 HindIII site (HindIII disrupted) of pTIF1B4, yielding pTIF1B7. The loxP-containing XhoI fragment of pTIF1B7 was then inserted into the XhoI site of pTIF1B11 to generate the final targeting vector (pTIF1B13, also called pTIF1 $\beta$ <sup>(NL:L)</sup> in Fig. 1A).

### ES cell selection

The targeting vector was linearized with ClaI, purified on sucrose gradient, and electroporated into 129/Sv H1 ES cells (Dierich and Dollé, 1997) as described (Lufkin et al., 1991). After selection with G418 (150  $\mu$ g/ml), neomycin-resistant clones were expanded, their genomic DNA was prepared, digested with BamHI and analyzed by Southern blotting with the 3' probe (a 1.2-kb DNA fragment obtained by PCR amplification with the oligonucleotides XN134: 5'-GGTTG-TATCTAGAACCACAT-3' and XF51: 5'-AAGGCTTCGGAGGGG-TATAG-3'). Positive clones for homologous recombination were further analyzed after EcoRV digestion with the 5' probe (a 1.5-kb EcoRI genomic fragment) and with a neomycin probe.

### Generation of mutant mice

ES cells bearing an L3 targeted allele (AO180 and AO122) were injected into C57BL/6 blastocysts. Chimeric mice were backcrossed with C57BL/6 mice, and germ-line transmission of the targeted allele was determined in the agouti offspring by PCR analysis using a sense primer located in intron 3 upstream to the 5' HindIII site (primer YD208, 5'-GGAATGGTTGTTTCATTGGTG-3'), and an antisense primer located downstream of the 5' loxP site in the PGK-Neo cassette (primer RR189, 5'-AAGCGCATGCTCCAGACTGC-3'). These primers generated a 180-bp DNA fragment from the targeted allele. Mice heterozygous for the targeted TIF1 $\beta$  gene (TIF1 $\beta$ <sup>+L3</sup>) were crossed with cytomegalovirus-Cre (CMV-Cre) transgenic mice (Dupé et al., 1997). Tail DNA of the offspring was analyzed by Southern blotting after EcoRV digestion and hybridization with the 5' probe. Mice positive for the presence of the deleted TIF1 $\beta$  allele (L<sup>-</sup>) were crossed with C57BL/6 mice to derive TIF1 $\beta$ <sup>+L-</sup> heterozygotes devoid of the Cre transgene and selected by genomic PCR using a mixture of three primers: sense primer (YD208), antisense primer (VR211, 5'-ACCTTGGCCCATTTATTGATAAAG-3') located in intron 3 downstream to the 3' HindIII site, and antisense primer (TV210, 5'-GCGAGCACGAATCAAGGTCAG-3') located in exon 16 (see Fig. 2A). Mice heterozygous for the TIF1 $\beta$  mutation were intercrossed to generate homozygotes. For the timing of embryo collection, the morning of the day of the vaginal plug was taken as E0.5. Genotypes were determined by Southern blotting and/or PCR on DNA extracted from tails (newborn and adult mice), from the yolk sac (E8.5 to E17.5 embryos), from the entire embryo (E3.5 to E8.0 embryos), or from paraffin-embedded sections as described in Zeitlin et al. (1995).

### Histological analysis

Decidua were collected in 10 mM phosphate-buffered saline (PBS), pH 7.2, then fixed in Bouin's fluid for 14 hours, dehydrated and embedded in paraffin. Serial sections were cut at 6  $\mu$ m and stained with Hematoxylin and Eosin.

### In situ hybridization

ISH with <sup>35</sup>S-labelled riboprobes was performed as described in Niederreither and Dollé (1998). The probes used included *Brachyury* (a kind gift from D. Herrmann, Freiburg University, Germany) and TIF1 $\beta$  (region +1168 to +1695 of the TIF1 $\beta$  cDNA; Le Douarin et al., 1996).

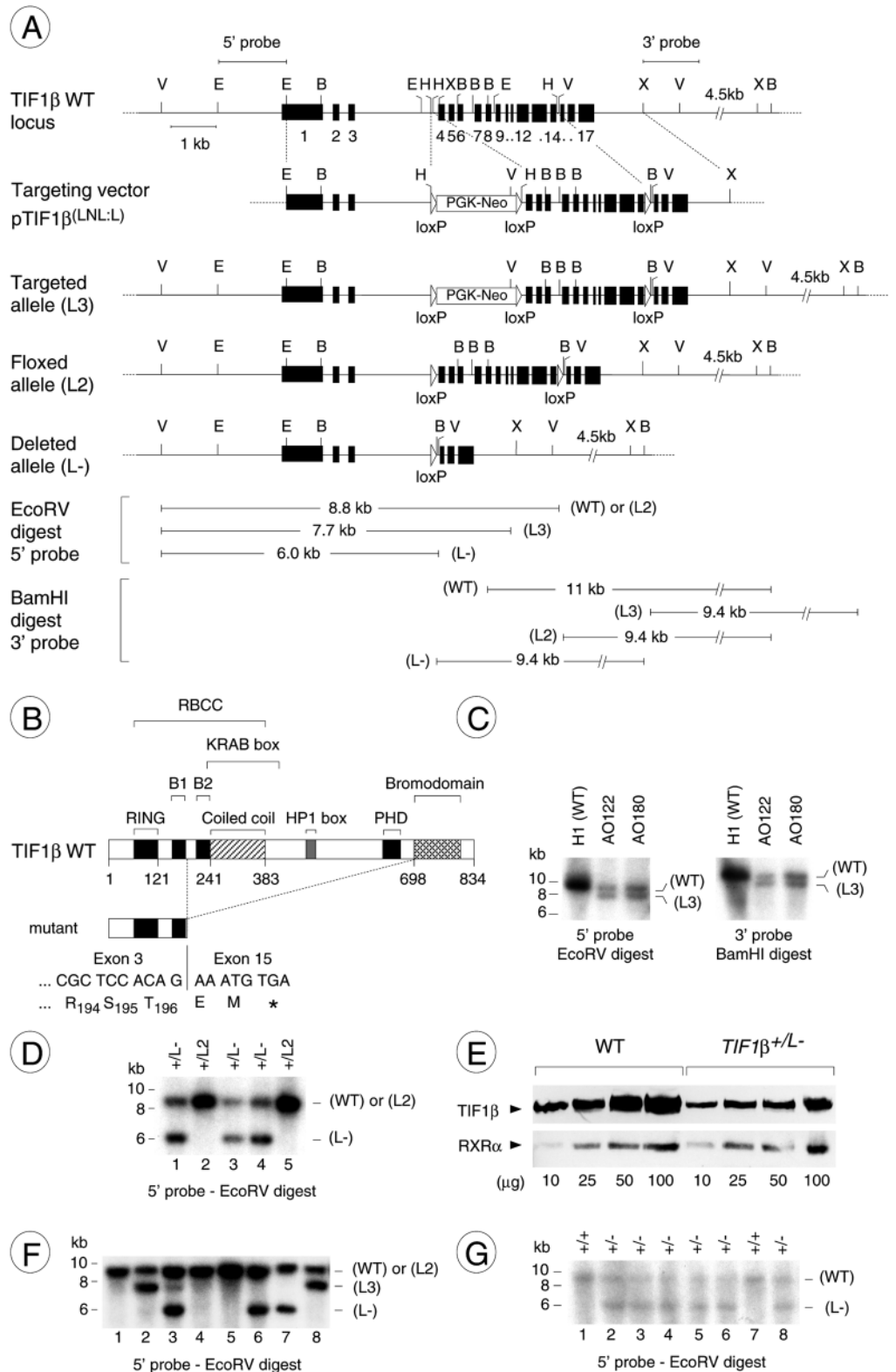
### Western blot analysis

Proteins from ES whole-cell extracts, prepared by three cycles of freeze-thaw in PBS containing 10% glycerol and a protease inhibitor cocktail, were separated on 8% gel by SDS-PAGE and electrotransferred onto nitrocellulose filters. The filters were incubated with specific antibodies followed by a peroxidase-conjugated anti-mouse IgG secondary antibody and developed using an ECL detection kit (Amersham Pharmacia Biotech.). Antibodies used include anti-TIF1 $\beta$  mAb (1Tb3), raised against recombinant *E. coli*-expressed mouse TIF1 $\beta$  (Nielsen et al., 1999), anti-TIF1 $\beta$  mAb (3Tb1H3), directed against TIF1 $\beta$  (amino acids 20-38) and anti-mRXX $\alpha$  polyclonal antibody, RPRX $\alpha$ (A) (Rochette-Egly et al., 1994).

### Whole-mount immunofluorescence

Preimplantation embryos from heterozygote intercrosses were flushed from uteri at E3.5, washed in PBS, fixed in freshly prepared 2% paraformaldehyde in PBS for 4 minutes, permeabilized with PBS containing 0.1% Triton X-100 twice for 5 minutes, and incubated with the anti-TIF1 $\beta$  mAb (1Tb3) overnight at room temperature. An irrelevant antibody (anti-Flag antibody 2FIIB4) was used as a negative control. Embryos were washed twice for 5 minutes in PBS-0.1% Triton X-100, followed by incubation for 1 hour at room temperature with Cy3 indocarbocyanine-conjugated goat anti-mouse IgG. They were stained for DNA with Hoechst 33258. The stained embryos were

**Fig. 1.** Targeted disruption of *TIF1 $\beta$*  using the Cre-loxP system. (A) Diagram showing the genomic map of *TIF1 $\beta$* , the targeting construct, and the targeted allele before (*L3*) and after (*L2* and *L-*) Cre-mediated excision of the selection cassette. Exons are represented as numbered boxes, introns as connecting lines. The three loxP sites (open triangles) and the *PGK-Neo* cassette are indicated. The 5' and 3' probes are 1.5 kb *EcoRI-EcoRI* fragment and 1.2 kb PCR fragment, respectively. The size of the DNA fragments expected with the 5' probe upon digestion with *EcoRV* and with the 3' probe upon digestion with *BamHI* are indicated. Relevant restriction sites: V, *EcoRV*; E, *EcoRI*; B, *BamHI*; H, *HindIII*; X, *XhoI*. (B) Schematic representation of wild type (WT) and mutant TIF1 $\beta$  proteins. The structural and functional domains are indicated (Le Douarin et al., 1996, 1998; Nielsen et al., 1999; Ryan et al., 1999). Numbers refer to amino acid positions (Le Douarin et al., 1996). The predicted product of the mutated *TIF1 $\beta$*  cDNA would correspond to a C-terminally truncated protein consisting of the first 196 amino acids of TIF1 $\beta$ . (C) Southern blot analysis of DNAs derived from wild-type (H1) and targeted (AO122 and AO180) ES cells. Genomic DNA was digested with *EcoRV* or *BamHI*, as indicated, blotted and hybridized with the 5' probe (left side) or the 3' probe (right side). (D) Southern blot analysis of DNAs from a series of ES cell clones derived from the AO180 *TIF1 $\beta$* <sup>+L3</sup> ES cell line transfected with the Cre-encoding expression plasmid PIC-Cre. Cre expression led to removal of the selection cassette, generating floxed (*L2*) and deleted (*L-*) alleles (see A). (E) TIF1 $\beta$  protein levels in wild type and *TIF1 $\beta$* <sup>+L-</sup> ES cells. Increasing amounts of whole-cell extracts (10 to 100  $\mu$ g protein) were analyzed by western blotting using the anti-TIF1 $\beta$  monoclonal antibody 1TB3, directed against the TIF1 $\beta$  carboxy terminus (amino acids 123-834), or the anti-RXR $\alpha$  polyclonal antibody RPRX $\alpha$ (A) (used as a control for the amount of protein extract loaded). (F) Southern blot analysis of representative tail DNA samples derived from 1-week-old offspring of crosses between heterozygous *TIF1 $\beta$* <sup>+L3</sup> mice and *CMV-Cre* transgenic mice. Incomplete excision of the loxP-flanked DNA sequences was observed in lane 3. (G) Southern blot analysis of tail DNA derived from 1-week-old offspring of heterozygous *TIF1 $\beta$* <sup>+L-</sup> intercrosses.



mounted and photographed with a Leica TCS4D fluorescence confocal microscope.

## RESULTS

### Targeted disruption of the mouse *TIF1 $\beta$* gene

A 7-kb genomic fragment containing the entire mouse *TIF1 $\beta$*  coding sequence (F. Cammas, J.-M. Garnier, P. Chambon and R. Losson, unpublished) was used to generate a targeting vector pTIF1 $\beta$ <sup>(LNL:L)</sup>, in which a *PGK-Neo* selection cassette flanked by two *loxP* sites was introduced into intron 3 and a *loxP* site inserted into intron 14 (Fig. 1A; see Materials and Methods for details). Upon homologous recombination and subsequent Cre-mediated excision, exons 4 to 14 of *TIF1 $\beta$*  together with the selection marker cassette are expected to be deleted, thereby causing a frameshift mutation with an immediate stop of translation in exon 15 (Fig. 1B). The predicted product of this mutated gene would correspond to a C-terminally truncated TIF1 $\beta$  protein lacking all functional domains beyond the B1 motif (Fig. 1B).

The targeting vector pTIF1 $\beta$ <sup>(LNL:L)</sup> was electroporated into 129/Sv H1 ES cells, and 273 G418-resistant clones were isolated, of which five (including AO122 and AO180) were found to be positive for homologous recombination by Southern blot analysis using 'outside' 5' and 3' probes (Fig. 1A,C). All of them carried a single-copy integration at the *TIF1 $\beta$*  locus as revealed by Southern blot analysis with a *Neo* probe (data not shown). One of these targeted ES cell lines (AO180) was transiently transfected with a Cre-encoding expression plasmid (PIC-Cre) to test whether a Cre-mediated excision of the targeted allele (*L3*) could be achieved. Clones, in which a complete excision of the *loxP*-flanked DNA sequences generated a deleted allele (*L-*; Fig. 1A), were isolated (Fig. 1D). The effect of this deletion on *TIF1 $\beta$*  gene expression was then assessed by western blot analysis, using whole cell extracts from wild type and *TIF1 $\beta$ <sup>+L-</sup>* ES cells. A single reacting species of the expected size for the TIF1 $\beta$  protein was detected with a monoclonal antibody against the carboxy-terminal end of TIF1 $\beta$  (see Materials and Methods, and Fig. 1E). The reactivity of this protein was decreased by half in the heterozygous ES cells, showing a dosage effect (Fig. 1E). No lower molecular mass species, which might correspond to a shortened translation product from the deleted allele, was detected with a monoclonal antibody raised against the amino terminus of TIF1 $\beta$  (see Materials and Methods; not shown). These results confirm that, as expected, the *TIF1 $\beta$ <sup>L-</sup>* allele is a null allele.

The two independent *TIF1 $\beta$ <sup>+L3</sup>* ES cell lines, AO122 and AO180, were injected into C57BL/6 blastocysts to produce

**Table 1. Genotype analysis of *TIF1 $\beta$ <sup>+L-</sup>* intercross progeny**

Stage	Genotype			Resorption	Total
	+/+	+/-	-/-		
Newborn	24	42	0	-	66
E17.5-8.5	14	35	0	16	65
E8.0	6	5	3*	2	16
E7.5	4	11	4*	1	20
E3.5	13	27	12	-	52

\*Embryos are either severely growth-retarded or being resorbed.

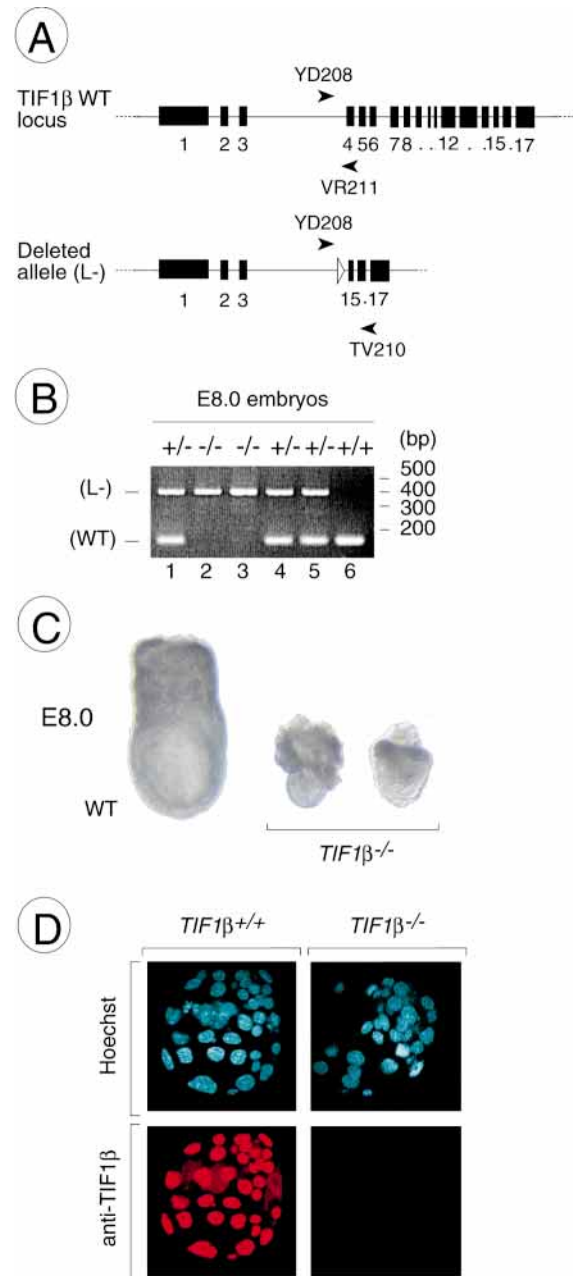


**Fig. 2.** Analysis of E8.0 wild type and *TIF1 $\beta$ <sup>-/-</sup>* mutant embryos, and TIF1 $\beta$  immunodetection in E3.5 wild type and mutant embryos. (A) PCR strategy for amplification of wild type (WT) and deleted (*L-*) *TIF1 $\beta$*  alleles. DNA samples were subjected to PCR amplification using a mixture of three primers (see Materials and Methods for sequences). PCR amplification of the wild-type *TIF1 $\beta$*  allele by sense and antisense primers YD208 and VR211 produces a 152-bp DNA fragment (B, lower band), while PCR amplification of the deleted allele by sense and antisense primers YD208 and TV210 produces a 390-bp DNA fragment (B, upper band). (B) Representative genotypic analysis of E8.0 embryos from a *TIF1 $\beta$ <sup>+L-</sup>* intercross. (C) Dissected wild type (left) and *TIF1 $\beta$ <sup>-/-</sup>* mutant (right) littermates at E8.0. (D) *TIF1 $\beta$*  detection in wild type (left) and *TIF1 $\beta$ <sup>-/-</sup>* E3.5 blastocysts. Upper panels show the Hoechst DNA staining, and lower panels correspond to immunodetection with anti-TIF1 $\beta$  antibody.

chimeric mice, and both contributed to the germ line. Mice heterozygous for the targeted *TIF1 $\beta$*  gene (*TIF1 $\beta$ <sup>+L3</sup>*) were crossed with *cytomegalovirus-Cre* transgenic mice (*CMV-Cre*) expressing the Cre recombinase under the control of the human *cytomegalovirus* promoter (Dupé et al., 1997). Tail DNA of the offspring was analyzed by Southern blot and genomic PCR to detect Cre-mediated excision (Fig. 1F, and data not shown). This cross led to the generation of mosaic animals, in which cells containing either nonexcised (*L3*) or excised (*L-*) DNA coexisted (see Fig. 1F, lane 3). These animals were crossed with wild-type C57BL/6 mice, and *TIF1 $\beta$ <sup>+L-</sup>* mice devoid of

the *CMV-Cre* transgene were selected, thereafter designated as *TIF1 $\beta$ <sup>+/-</sup>*.

### TIF1 $\beta$ is essential for early postimplantation development

Mice heterozygous for the *TIF1 $\beta$*  mutation were viable and fertile. Genotype analysis of progeny from heterozygote intercrosses revealed that 36% were wild type, 64% heterozygous, and none homozygous (Fig. 1G and Table 1), indicating that the *TIF1 $\beta$*  null mutation was recessive embryonic lethal.

To determine the time of embryonic lethality, embryos from heterozygote intercrosses were collected at different times of gestation and genotyped (Table 1). No homozygous mutant embryos were recovered at, or after, E8.5 (Table 1), and the percentage of resorptions at these times was unusually high (25%; Table 1). At E8.0 and E7.5, *TIF1 $\beta$ <sup>-/-</sup>* mutants were identified by PCR (Table 1 and Fig. 2A,B). These mutants were either severely growth-retarded or undergoing resorption (Fig. 2C and data not shown).

When preimplantation embryos (morulae and blastocysts) collected by uterine flushing at E3.5 were examined and genotyped, we found 23% (12/52) homozygous null embryos that were indistinguishable from heterozygous and wild-type embryos (Table 1). These E3.5 embryos were examined for the presence of TIF1 $\beta$  protein using whole-mount immunofluorescence. Almost all nuclei of wild-type blastocysts, in both the inner cell mass and the trophectoderm, were found to express TIF1 $\beta$  (Fig. 2D). In contrast, no TIF1 $\beta$  staining was detected above background level in null blastocysts (Fig. 2D), suggesting that the survival of these embryos is not due to the persistence of a maternal pool of TIF1 $\beta$  protein. Taken together, results of this retrograde genotypic analysis indicate that TIF1 $\beta$  plays a critical role in early postimplantation development and is most probably non-essential for preimplantation cell viability.

### TIF1 $\beta$ <sup>-/-</sup> mutant embryos do not undergo gastrulation

Histological sections of embryos from heterozygote intercrosses were analyzed at several developmental stages. At E5.5 no overt abnormalities were found in a total of 39 embryos. The earliest defects were observed at E6.5 and E7.0 in 23% (5 out of 21) of the embryos. Importantly, these defects were not found in embryos from wild-type crosses or *TIF1 $\beta$ <sup>+/-</sup>*/wild-type intercrosses.

In normal E6.5-E7.0 embryos, the proamniotic cavity (pa, Fig. 3A,C) has formed, and the primitive embryonic ectoderm (ee) and primitive extraembryonic ectoderm (ex) are

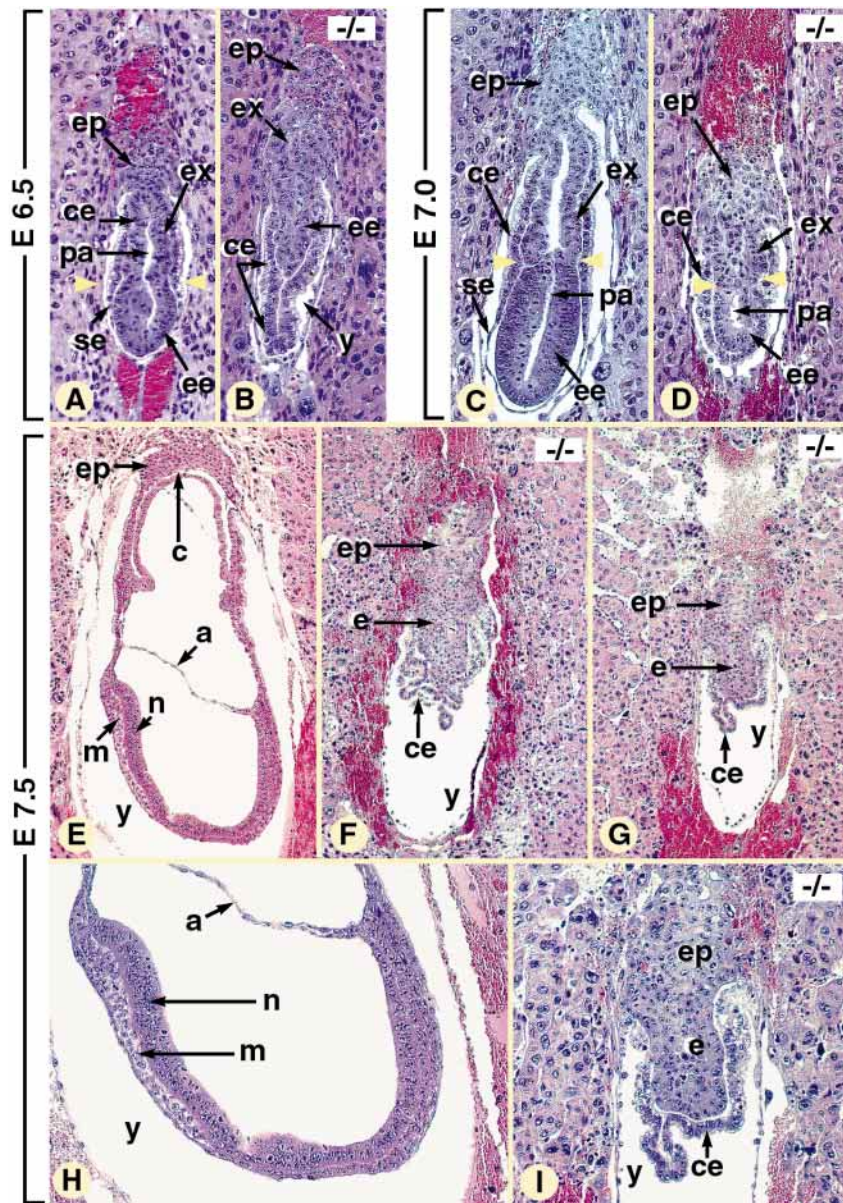


**Fig. 3.** Histological sections of normal (A,C,E,H) and presumptive *TIF1 $\beta$ <sup>-/-</sup>* (B,D,F,G,I) embryos at E6.5 (A,B), E7.0 (C,D) and E7.5 (E-I). a, amnion; c, ectoplacental cavity; ce, cuboidal visceral endoderm; e, ectoderm; ee, embryonic ectoderm; ep, ectoplacental cone; ex, extraembryonic ectoderm; m, embryonic mesoderm; n, neuroectoderm; pa, proamniotic cavity; se, squamous visceral endoderm; y, yolk sac cavity. Arrowheads in A, C and D indicate the position of the circular furrow.  $\times 50$  (A-D,H,I);  $\times 25$  (E-G).

separated by a circular furrow (yellow arrowheads in Fig. 3A,C). The visceral endodermal cells, which are in close

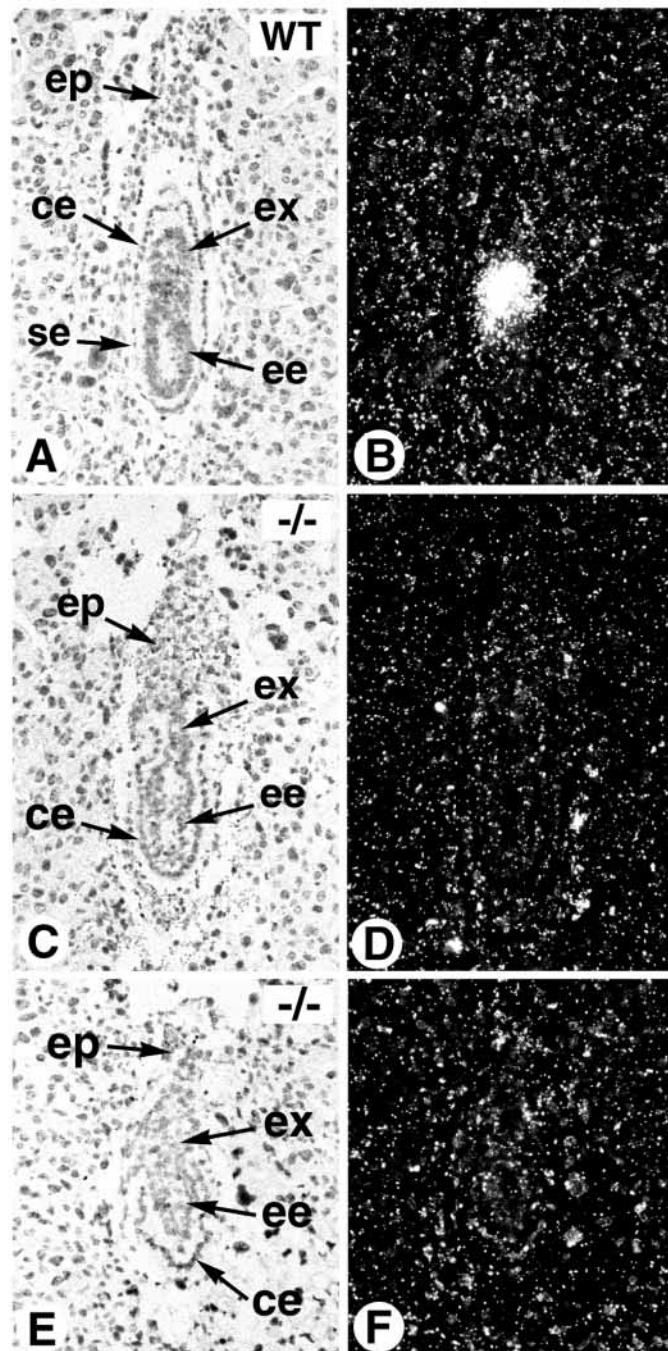


**Fig. 4.** In situ hybridization analysis of *Brachyury* expression in wild type (WT) (A,B) and *TIF1β*<sup>-/-</sup> (C-F) littermate embryos collected at E 7.0. (B,D,F) are dark-field views of (A,C,E), respectively, and show the hybridization signal grains as white dots. Mutant embryos were identified by the cuboidal appearance of the entire visceral endoderm layer, and their genotype was confirmed by PCR analysis. The control embryo (A,B) shows a strong signal at the embryonic/extraembryonic junction (i.e the early primitive streak), in contrast to the null embryos which only exhibit background grain. ce, cuboidal visceral endoderm; ee, embryonic ectoderm; ep, ectoplacental cone; ex, extraembryonic ectoderm; se, squamous visceral endoderm.  $\times 100$ .

contact with the ectodermal cells, can be subdivided into distinct subpopulations: squamous cells surrounding the embryonic ectoderm (se, Fig. 3A,C) and cuboidal cells, with characteristic apical vacuoles, surrounding the extraembryonic ectoderm (ce, Fig. 3A,C). Abnormal presumptive *TIF1β*<sup>-/-</sup> embryos at E6.5 (Fig. 3B) and E7.0 (Fig. 3D) were small in size; their proamniotic cavity was barely distinguishable (pa, Fig. 3D) or was absent (Fig. 3B). The frontier between the embryonic and extraembryonic ectoderms was poorly defined (arrowheads in Fig. 3D). The ectoderm, notably its embryonic portion, contained fewer cells than in control embryos (compare Fig. 3C,D). The visceral endoderm consisted exclusively of cuboidal, vacuolated cells, as it is normally the case in E5.5 embryos. Moreover, the presumptive mutant endoderm formed large folds, protruding into the yolk sac cavity (y, Fig. 3B), as if the growth of this tissue continued in the absence of expansion of the overlying primitive ectoderm.

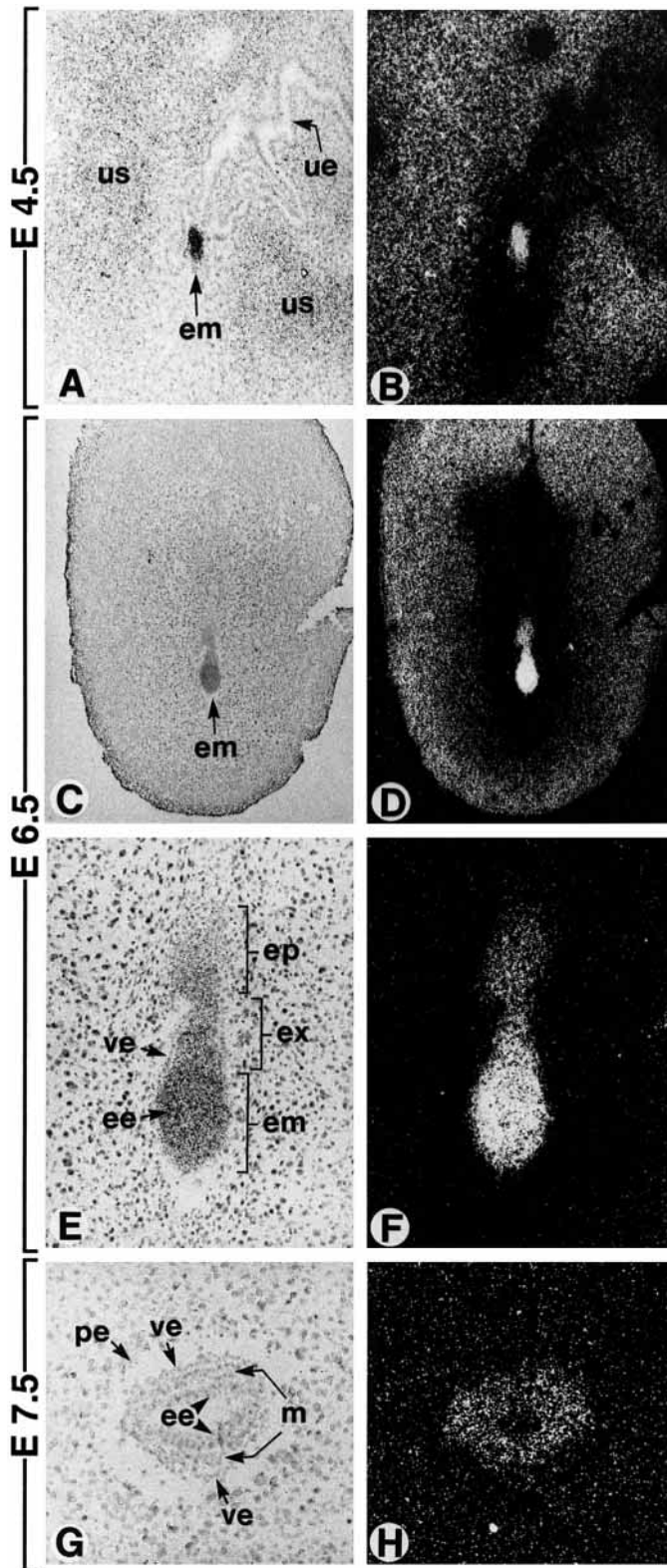
At E7.5, control embryos have formed mesoderm (m, Fig. 3E,H) and neurectoderm (n, Fig. 3E,H), as a consequence of gastrulation. Moreover, their extraembryonic ectoderm has organized into an ectoplacental cavity (c, Fig. 3) and amnion (a, Fig. 3E,H). The three presumptive E7.5 *TIF1β*<sup>-/-</sup> embryos (collected in a litter of 12 embryos) were still alive as assessed by the presence of mitotic figures and absence of large numbers of picnotic nuclei. However, they had not progressed in their development. In particular, they never contained mesodermal cells, their extraembryonic ectoderm was not organized and the visceral endoderm did not differentiate into the squamous cell type (Fig. 3F,G,I).

To further investigate whether mesoderm induction takes place in *TIF1β*<sup>-/-</sup> embryos, we examined the expression of the gene *Brachyury*, an early marker of the mesoderm lineage, by in situ hybridization (ISH) on sections of embryos collected at E7.0 and genotyped by PCR (Zeitlin et al., 1995). All heterozygous and wild-type embryos analyzed ( $n=10$ ) exhibited the expected expression of *Brachyury* in the posterior part of the egg cylinder, defining the early primitive streak (Fig. 4A,B, and data not shown). However, no *Brachyury* expression was detected in three *TIF1β*<sup>-/-</sup> embryos (Fig. 4C-F and data not shown), including one mutant embryo whose size was comparable to that of its control littermates (Fig. 4C,D).

Altogether, these results show that *TIF1β* is required for egg-cylinder organization and mesoderm induction, and that in its absence, development cannot progress further than the E5.5 stage.

#### ***TIF1β* expression during early mouse development**

The early postimplantation defects of the *TIF1β*<sup>-/-</sup> embryos prompted us to examine the pattern of *TIF1β* expression before and during gastrulation by ISH. In agreement with the detection of the *TIF1β* protein in preimplantation E3.5 blastocysts (Fig. 2D), high expression levels of *TIF1β* transcripts were detected in E4.5 implanting embryos (Fig. 5A,B). A weaker ISH signal was seen in uterine stromal cells, while the uterine epithelium was not labelled (Fig. 5A,B). A similar expression pattern was observed in early postimplantation embryos at E5.0 and E5.5 (data not shown). At E6.5, *TIF1β* transcripts continued to be highly expressed in the embryonic ectoderm (ee, Fig. 5C-F). Lower expression was seen in the extraembryonic ectoderm (ex, Fig. 5E,F) and in the ectoplacental cone (ep, Fig. 5E,F). Furthermore, the visceral



endoderm layer exhibited little, if any, labelling (ve, Fig. 5E,F). At E7.5, *TIF1 $\beta$*  expression was detected throughout the ectodermal and mesodermal (m) layers, but not the parietal (pe) or visceral endoderm, of the embryos (Fig. 5G,H, and data not shown). Thus, *TIF1 $\beta$*  appears to be highly expressed in E4.5–E6.5 postimplantation embryos prior to gastrulation.

**Fig. 5.** In situ hybridization analysis of *TIF1 $\beta$*  expression during early mouse development. Selected sections are displayed under bright-field (left) and dark-field (right) illumination, revealing the signal grain in white. (A,B) E4.5 embryo within the uterine lumen. (C,D) Overview of an implantation site at E6.5. (E,F) High-power magnification of the same conceptus. (G,H) Transverse section of an E7.5 embryo. ee, embryonic ectoderm; em, embryo; ep, ectoplacental cone; ex, extraembryonic region; m, mesoderm; pe, parietal endoderm; ue, uterine epithelium; us, uterine stroma; ve, visceral endoderm.  $\times 100$  (A,B,E–H);  $\times 40$  (C,D).

## DISCUSSION

We have examined the developmental consequences of a null mutation in the *TIF1 $\beta$*  gene and found that *TIF1 $\beta$* -deficient embryos implant in the uterine wall, but arrest in their development just prior to gastrulation and are completely resorbed by E8.5, indicating that TIF1 $\beta$  exerts cellular function(s) essential for early postimplantation development.

The earliest stage at which morphologically abnormal embryos were identified in heterozygote intercrosses is E6.5, which corresponds to the onset of gastrulation. Abnormal *TIF1 $\beta$* <sup>-/-</sup> embryos showed a reduced cell number in the embryonic ectoderm, no evidence of mesoderm formation, and an altered morphology in their visceral endoderm that fails to acquire the flattened morphology normally appearing at the early gastrulation stage. Interestingly, a lack of the squamous cell population of visceral endoderm is also associated with embryonic defects in null mutants for the *TGF $\beta$* -related gene *nodal* (Iannaccone et al., 1992), the type I activin receptor *ActRIB* gene (Gu et al., 1998), the EGF-CFC family gene *Cripto* (Ding et al., 1998), the tumor suppressor gene *SMAD2* (Weinstein et al., 1998) and the X-ray cross-complementing *Xrcc1* gene (Tebbs et al., 1999). The molecular basis of this abnormal endodermal phenotype is unknown. The finding that this abnormality was retained in a number of *Xrcc1/Trp53* double-mutant embryos, which initiated gastrulation, indicates that it does not result from a defect in initiation of gastrulation (Tebbs et al., 1999). However, it may be the consequence of a non-cell-autonomous effect in the case of *nodal* (Conlon et al., 1994), *ActRIB* (Gu et al., 1998) and *Cripto* (Ding et al., 1998) mutants, as these genes are not expressed in visceral endoderm at the early gastrulation stage. Similarly, the abnormal endodermal phenotype of *TIF1 $\beta$*  null mutants may reflect a non-cell-autonomous defect, as *TIF1 $\beta$*  transcripts do not appear to be expressed in visceral endoderm, as judged from ISH experiments. Studies with chimeric embryos are required to determine whether the primary defect of the *TIF1 $\beta$*  mutation is of embryonic or extraembryonic origin.

In agreement with our *TIF1 $\beta$*  expression data in ES cells, the TIF1 $\beta$  protein could be revealed in preimplantation embryos at the blastocyst stage (E3.5). As it could not be detected in *TIF1 $\beta$* <sup>-/-</sup> blastocysts, its synthesis must correspond to an early event in mouse embryogenesis. Note that even though they do not contain any detectable TIF1 $\beta$  protein, the mutant blastocysts are morphologically indistinguishable from their wild-type littermates. Moreover, they are able to hatch from the zone pellucida, adhere and develop trophoblastic giant cells after 4 days of outgrowth (our unpublished results). Thus, *TIF1 $\beta$*  is not required for cell viability at preimplantation stages.

*TIF1 $\beta$*  belongs to the family of *TIF1* genes whose physiological functions are unknown (Le Douarin et al., 1996; see Introduction). Our present data provides the first demonstration that a member of this family plays an essential function in vivo. Our study also provides genetic evidence that, at least during early embryogenesis, the members of this family, though structurally related, exert distinct, non-redundant functions. Based on biochemical and transient cotransfection data, *TIF1 $\beta$* , but neither *TIF1 $\alpha$*  nor *TIF1 $\gamma$* , was reported to interact with and act as a corepressor for several members of the KRAB-ZFP family (Friedman et al., 1996; Kim et al., 1996; Moosmann et al., 1996; Venturini et al., 1999; Nielsen et al., 1999; see Introduction). Whether the embryonic lethality of *TIF1 $\beta$* <sup>-/-</sup> embryos could be related to a failure of KRAB-ZFP-mediated silencing is unknown, but strongly suggested by several lines of evidence that point to an important role of the *KRAB-ZFP* gene family in regulating cell differentiation and development. A number of KRAB-ZFPs have been shown to exhibit temporally and spatially regulated expression patterns, at specific stages of development (Lange et al., 1995; Shannon and Stubbs, 1999), in germ cells (Bellefroid et al., 1998; Ogawa et al., 1998), in hematopoietic lineages (Mark et al., 1999; Liu et al., 1999), as well as in a limited number of organs (Witzgall et al., 1993; Mazarakis et al., 1996; Tekki-Kessaris et al., 1999). Moreover, several *KRAB-ZFP* genes have been involved in human diseases on the basis of their chromosomal location (Mannens et al., 1996; Dreyer et al., 1998; Rippe et al., 1999), or associated with embryonic lethal mutations (Shannon and Stubbs, 1999). In view of their possible important biological functions and their abundance in the genome, a dysfunction of KRAB-ZFPs may underlie the severe mutant phenotype of *TIF1 $\beta$* -deficient embryos.

In summary, we have shown that *TIF1 $\beta$*  is essential for the development of the mouse embryo at the egg-cylinder stage and for subsequent gastrulation. That *TIF1 $\beta$*  may have additional role(s) during and after gastrulation is suggested by its persistent expression during late embryogenesis and adult life (our unpublished results; Kim et al., 1996). Conditional knockouts of *TIF1 $\beta$*  at specific developmental stages and in specific tissues are in progress to investigate this possibility.

We are grateful to R. Lorentz, J.-M. Bornert, P. Unger, B. Weber, I. Tilly and C. Hummel, as well as the staff of ES cell culture and animal facility, for their excellent technical assistance. We also thank D. Metzger, M. Oulad-Abdelghani, A. Perea-Gomez, M. Rhinn and J. Brocard for material gifts, technical advice and helpful discussions, N. Messadeq for confocal microscopy, J.-L. Vonesh and D. Hentsch for optical microscopy, S. Vicaire and D. Stephan for sequencing constructs and A. Staub and F. Ruffenach for oligonucleotide synthesis. This work was supported by the Centre National de la Recherche Scientifique, the Institut National de la Santé et de la Recherche Médicale, the Hôpitaux Universitaires de Strasbourg, the association pour la Recherche sur le Cancer, the Collège de France, the Fondation pour la Recherche Médicale and Bristol-Myers-Squibb. F.C. was supported by a fellowship from the Ligue contre le cancer.

## REFERENCES

Aasland, R., Gibson, T. J. and Stewart, A. F. (1995). The PHD finger: implication for chromatin-mediated transcriptional regulation. *Trends Biochem. Sci.* **20**, 56-59.

- Agata, Y., Matsuda, E. and Shimizu, A. (1999). Two novel Krüppel-associated box-containing zinc-finger proteins, KRAZ1 and KRAZ2, repress transcription through functional interaction with the corepressor KAP-1 (TIF1 $\beta$ /KRIP-1). *J. Biol. Chem.* **274**, 16412-16422.
- Bellefroid, E. J., Poncelet, D. A., Lecocq, P. J., Revelant, O. and Martial, J. A. (1991). The evolutionary conserved Krüppel-associated box domain defines a subfamily of eukaryotic multifingered proteins. *Proc. Natl. Acad. Sci. USA* **88**, 3608-3612.
- Bellefroid, E. J., Sahin, M., Poncelet, D. A., Riviere, M., Bourguignon, C., Martial, J. A., Morris, P. L., Pieler, P., Szpirer, C. and Ward, D. C. (1998). Kzf1 – a novel KRAB zinc finger protein encoding gene expressed during rat spermatogenesis. *Biochim. Biophys. Acta* **1398**, 321-329.
- Boddy, M. N., Duprez, E., Borden, K. L. B. and Freemont, P. S. (1997). Surface residue mutations of the PML RING finger domain alter the formation of nuclear matrix-associated PML bodies. *J. Cell Sci.* **110**, 2197-2205.
- Carroll, S. B. (1990). Zebra patterns in fly embryos: activation of stripes or repression of interstripes. *Cell* **60**, 9-16.
- Cocktell, M. and Gasser, S. (1999). Nuclear compartments and gene regulation. *Curr. Opin. Genet. Dev.* **9**, 199-205.
- Conlon, F. L., Lyons, K. M., Takaesu, N., Barth, K. S., Kispert, A., Herrmann, B. and Roberston, E. J. (1994). A primitive requirement for nodal in the formation and maintenance of the primitive streak in the mouse. *Development* **120**, 1919-1928.
- Deuschle, U., Meyer, W. K. and Thiesen, H.-J. (1995). Tetracycline-reversible silencing of eukaryotic promoters. *Mol. Cell Biol.* **15**, 1907-1914.
- Dhalluin, C., Carlson, J. E., Zeng, L., He, C., Aggarwal, A. K. and Zhou, M.-M. (1999). Structure and ligand of a histone acetyltransferase bromodomain. *Nature* **399**, 491-496.
- Dierich, A. and Dollé, P. (1997). Gene targeting in embryonic stem cells. In *Methods in Developmental Toxicology and Biology* (ed. S. Klug and R. Thiel), pp. 111-123. Germany: Blackwell Science Ltd.
- Ding, J., Yang, L., Yan, Y.-T., Chen, A., Desai, N., Wynshaw-Boris, A. and Shen, M. M. (1998). Cripto is required for correct orientation of the anterior-posterior axis in the mouse embryo. *Nature* **395**, 702-707.
- Dreyer, S. D., Zhou, L., Machado, M. A., Horton, W. A., Zabel, B., Winterpacht, A. and Lee, B. (1998). Cloning, characterization, and chromosomal assignment of the human ortholog of murine Zfp-37, a candidate gene for Nager syndrome. *Mamm. Genome* **9**, 458-462.
- Dupé, V., Davenne, M., Brocard, J., Dolle, P., Mark, M., Dierich, A., Chambon, P. and Rijli, F. M. (1997). In vivo functional analysis of the Hoxa-1 3' retinoic acid response element (3'RARE). *Development* **124**, 399-410.
- Eissenberg, J. C., Elgin, S. C. R. and Paro, P. (1995). Epigenetic regulation in *Drosophila*: a conspiracy of silence. In *Chromatin Structure and Gene Expression*, Frontiers in Molecular Biology (ed. S. C. R. Elgin), pp. 147-171. Oxford, UK: Oxford University Press.
- Elgin, S. C. R. (1996). Heterochromatin and gene regulation in *Drosophila*. *Curr. Opin. Genet. Dev.* **6**, 193-202.
- Fisher, A. L. and Caudy, M. (1998). The function of Hairy-related bHLH proteins in cell fate decisions. *BioEssays* **20**, 298-306.
- Friedman, J. R., Fredericks, W. J., Jensen, D. E., Speicher, D. W., Huang, X.-P., Neilson, E. G. and Rauscher III, F. J. (1996). KAP-1, a novel corepressor for the highly conserved KRAB repression domain. *Genes Dev.* **10**, 2067-2078.
- Gray, S. and Levine, M. (1996). Transcriptional repression in development. *Curr. Opin. Cell Biol.* **8**, 358-364.
- Gu, Z., Nomura, M., Simpson, B. B., Lei, H., Feijen, A., van den Eijnden-van Raaij, J., Donahoe, P. K. and Li, E. (1998). The type I activin receptor ActRIB is required for egg cylinder organization and gastrulation in the mouse. *Genes Dev.* **12**, 844-857.
- Iannaccone, P. M., Zhou, X., Khokha, M., Boucher, D. and Kuehn, M. R. (1992). Insertional mutation of a gene involved in growth regulation of the early mouse embryo. *Dev. Dyn.* **194**, 198-208.
- Ip, Y. T. and Hemavathy, K. (1997). *Drosophila* development: Delimiting patterns by repression. *Curr. Biol.* **7**, R216-R218.
- Jeanmougin, F., Wurtz, J.-M., Le Douarin, B., Chambon, P. and Losson, R. (1997). The bromodomain revisited. *Trends Biochem. Sci.* **22**, 151-153.
- Kim, S.-S., Chen, Y.-M., O'Leary, E., Witzgall, R., Vidal, M. and Bonventre, J. V. (1996). A novel member of the RING finger family, KRIP-1, associates with the KRAB-A transcriptional repressor domain of zinc finger proteins. *Proc. Natl. Acad. Sci. USA* **93**, 15299-15304.
- Kornberg, R. D. and Lorch, Y. (1999). Chromatin-modifying and -remodeling complexes. *Curr. Opin. Genet. Dev.* **9**, 148-151.

- Lange, R., Christoph, A., Thiesen, H.-J., Vopper, G., Johnson, K. R., Lemaire, L., Plomann, M., Cremer, H., Barthels, D. and Heinlein, U. A. (1995). Developmentally regulated mouse gene NK10 encodes a zinc finger repressor protein with differential DNA-binding domains. *DNA Cell Biol.* **14**, 971-81.
- Le Douarin, B., Zechel, C., Garnier, J.-M., Lutz, Y., Tora, L., Pierrat, B., Heery, D., Gronemeyer, H., Chambon, P. and Losson, R. (1995). The N-terminal part of TIF1, a putative mediator of the ligand-dependent activation function (AF-2) of nuclear receptors, is fused to B-raf in the oncogenic protein T18. *EMBO J.* **14**, 2020-2033.
- Le Douarin, B., Nielsen, A. L., Garnier, J.-M., Ichinose, H., Jeanmougin, F., Losson, R. and Chambon, P. (1996). A possible involvement of TIF1 $\alpha$  and TIF1 $\beta$  in the epigenetic control of transcription by nuclear receptors. *EMBO J.* **15**, 6701-6715.
- Le Douarin, B., You, J., Nielsen, A. L., Chambon, P. and Losson, R. (1998). TIF1 $\alpha$ : a possible link between KRAB zinc finger proteins and nuclear receptors. *J. Steroid Biochem. Mol. Biol.* **65**, 43-50.
- Liu, C., Levenstein, M., Chen, J., Tsofrina, E., Yonescu, R., Griffin, C., Civin, C. J. and Small, D. (1999). SZF1: a novel KRAB-zinc finger gene expressed in CD34+ stem/progenitor cells. *Exp. Hematol.* **27**, 313-325.
- Lufkin, T., Dierich, A., Le Meur, M., Mark, M. and Chambon, P. (1991). Disruption of the Hox-1.6 homeobox gene results in defects in a region corresponding to its rostral domain of expression. *Cell* **66**, 1105-1119.
- Mannens, M., Alders, M., Redeker, B., Blik, J., Steenman, M., Wiesmeyer, C., de Meulemeester, M., Ryan, A., Kalikin, L., Voute, T., De Kraker, J., Hoovers, J., Slater, R., Feinberg, A., Little, P. and Westerveld, A. (1996). Positional cloning of genes involved in the Beckwith-Wiedemann syndrome, hemihypertrophy, and associated childhood tumors. *Med. Pediatr. Oncol.* **27**, 490-494.
- Margolin, J. F., Friedman, J. R., Meyer, W. L.-H., Vissing, H., Thiesen, H.-J. and Rauscher III, F. J. (1994). Krüppel-associated boxes are potent transcriptional repression domains. *Proc. Natl. Acad. Sci. USA* **91**, 4509-4513.
- Mark, C., Abrink, M. and Hellman, L. (1999). Comparative analysis of KRAB zinc finger proteins in rodents and man: evidence for several evolutionarily distinct subfamilies of KRAB zinc finger genes. *DNA Cell Biol.* **18**, 391-396.
- Mazarakis, N., Michalovich, D., Karis, A., Grosveld, F. and Galjart, N. (1996). Zfp-37 is a member of the KRAB zinc finger gene family and is expressed in neurons of the developing and adult CNS. *Genomics* **33**, 247-57.
- Moosmann, P., Georgiev, O., Le Douarin, B., Bourquin, J.-P. and Schaffner, W. (1996). Transcriptional repression by RING finger protein TIF1 $\beta$  that interacts with the KRAB repression domain of KOX1. *Nucleic Acids Res.* **24**, 4859-4867.
- Moosmann, P., Georgiev, O., Thiesen, H.-J., Haggmann, M. and Schaffner, W. (1997). Silencing of RNA polymerases II and III-dependent transcription by the KRAB protein domain of KOX1. *Biol. Chem.* **378**, 669-677.
- Niederreither, K. and Dollé, P. (1998). In situ hybridization with <sup>35</sup>S-labeled probes for retinoid receptors. *Methods Mol. Biol.* **89**, 247-267.
- Nielsen, A. L., Ortiz, J. A., You, J., Oula-Abdelghani, M., Khechumian, R., Gansmuller, A., Chambon, P. and Losson, R. (1999). Interaction with members of the heterochromatin protein 1 (HP1) family and histone deacetylation are differentially involved in transcriptional silencing by members of the TIF1 family. *EMBO J.* **18**, 6385-6395.
- Ogawa, T., Poncelet, D. A., Kinoshita, Y., Noce, T., Takeda, M., Kawamoto, K., Udagawa, K., Lecocq, P. J., Marine, J. C., Martial, J. A. and Hosaka, M. (1998). Enhanced expression in seminoma of human zinc finger genes located on chromosome 19. *Cancer Genet. Cytogenet.* **100**, 36-42.
- Ogbourne, S. and Antalis, T. M. (1998). Transcriptional control and the role of silencers in transcriptional regulation in eukaryotes. *Biochem. J.* **331**, 1-14.
- Orphanides, G., Lagrange, T. and Reinberg, D. (1996). The general transcription factors of RNA polymerase II. *Genes Dev.* **10**, 2657-2683.
- Pengue, G., Calabro, V., Bartoli, P. C., Paggiuca, A. and Lania, L. (1994). Repression of transcriptional activity at a distance by the evolutionary conserved KRAB domain present in a subfamily of zinc finger proteins. *Nucleic Acids Res.* **22**, 2908-2914.
- Rippe, V., Belge, G., Meiboom, M., Kazmierczak, B., Fusco, A. and Bullerdiek, J. (1999). A KRAB zinc finger protein gene is the potential target of 19q13 translocation in benign thyroid tumors. *Genes Chromosomes Cancer* **26**, 229-236.
- Rochette-Egly, C., Lutz, Y., Pfister, V., Heiberger, S., Scheuer, I., Chambon, P. and Gaub, M.-P. (1994). Detection of retinoid X receptors using specific monoclonal and polyclonal antibodies. *Biophys. Biochem. Res. Commun.* **204**, 525-536.
- Ryan, R. F., Schultz, D. C., Ayanathan, K., Singh, P. B., Friedman, J. R., Fredericks, W. J. and Rauscher III, F. J. (1999). KAP-1 corepressor protein interacts and colocalizes with heterochromatic and euchromatic HP1 proteins: a potential role for Krüppel-associated box-zinc finger proteins in heterochromatin-mediated gene silencing. *Mol. Cell Biol.* **19**, 4366-4378.
- Saurin, A. J., Borden, K. L. B., Boddy, M. N. and Freemont, P. S. (1996). Does this have a familiar RING? *Trends Biochem. Sci.* **21**, 208-214.
- Schoenherr, C. J. and Anderson, D. J. (1995). The neuron-restrictive silencer factor (NRSF): A coordinate repressor of multiple neuron-specific genes. *Science* **267**, 1360-1363.
- Shannon, M. and Stubbs, L. (1999). Molecular characterization of Zfp54, a zinc-finger-containing gene that is deleted in the embryonic lethal mutation tw18. *Mamm. Genome* **10**, 739-743.
- Tebbs, R. S., Flannery, M. L., Meneses, J. J., Hartmann, A., Tucker, J. D., Thompson, L. H., Cleaver, J. E. and Pedersen, R. A. (1999). Requirement for the Xrcc1 DNA base excision repair gene during early mouse development. *Dev. Biol.* **208**, 513-529.
- Tekki-Kessarlis, N., Bonventre, J. V. and Boulter, C. A. (1999). Characterization of the mouse kid1 gene and identification of a highly related gene, kid2. *Gene* **240**, 13-22.
- Venturini, L., You, J., Stadler, M., Galien, R., Lallemand, V., Koken, M. H. M., Mattei, M. G., Ganser, A., Chambon, P., Losson, R. and de Thé, H. (1999). TIF1 $\gamma$ , a novel member of the transcriptional intermediary factor 1 family. *Oncogene* **18**, 1209-1217.
- Weinstein, M., Yang, X., Li, C., Xu, X., Gotay, J. and Deng, C.-X. (1998). Failure of egg cylinder elongation and mesoderm induction in mouse embryos lacking the tumor suppressor smad2. *Proc. Natl. Acad. Sci. USA* **95**, 9378-9383.
- Winston, F. and Allis, C. D. (1999). The bromodomain: a chromatin-targeting module? *Nature Struct. Biol.* **6**, 601-604.
- Witzgall, R., O'Leary, E., Gessner, R., Ouellette, A. J. and Bonventre, J. V. (1993). Kid-1, a putative renal transcription factor: regulation during ontogeny and in response to ischemia and toxic injury. *Mol. Cell Biol.* **13**, 1933-42.
- Witzgall, R., O'Leary, E., Leaf, A., Önalidi, D. and Bonventre, J. V. (1994). The Krüppel-associated box-A (KRAB-A) domain of zinc finger proteins mediates transcriptional repression. *Proc. Natl. Acad. Sci. USA* **91**, 4514-4518.
- Zazopoulos, E., Lalli, E., Stocco, D. M. and Sassone-Corsi, P. (1997). DNA binding and transcriptional repression by DAX-1 blocks steroidogenesis. *Nature* **390**, 311-315.
- Zeitlin, S., Liu, J. P., Chapman, D. L., Papaioannou, V. E. and Efstratiadis, A. (1995). Increased apoptosis and early embryonic lethality in mice nullizygous for the Huntington's disease gene homologue. *Nature Genet.* **11**, 155-163.
- Zhong, S., Delva, L., Rachez, C., Canciarelli, C., Gandini, D., Zhang, H., Kalantry, S., Freedman, L. P. and Pandolfi, P. P. (1999). A RA-dependent, tumor-growth suppressive transcription complex is the target of the PML-RAR $\alpha$  and T18 oncoproteins. *Nature Genet.* **23**, 287-295.